RSC Advances

PAPER

View Article Online
View Journal | View Issue

Cite this: *RSC Adv.*, 2016, **6**, 69930

Degradable polyurethane with poly(2-ethyl-2-oxazoline) brushes for protein resistance†

Jinxian Yang,[a] Lianwei Li,[a] Chunfeng Ma[b] and Xiaodong Ye*[a]

Received 26th May 2016
Accepted 16th July 2016

DOI: 10.1039/c6ra13663j

www.rsc.org/advances

Linear poly(2-ethyl-2-oxazoline) (PEtOx) with two hydroxyl groups located at the ends of each chain [PEtOx(OH)$_2$] was synthesized by cationic ring-opening polymerization (CROP) using 2,2-bis(hydroxymethyl)propionic acid as the end-capping agent. Further co-polycondensation of PEtOx and poly(ε-caprolactone) (PCL) led to degradable polyurethane-*graft*-poly(2-ethyl-2-oxazoline) (PU-*g*-PEtOx) with PCL as the soft segment. The structures of PU-*g*-PEtOx with different graft densities of PEtOx as well as different chain lengths were confirmed by various characterization techniques. Moreover, protein resistance experiments were examined by a quartz crystal microbalance with dissipation (QCM-D). The results demonstrated that the adsorption of three model proteins decreased with the increase in chain length of PEtOx when PU-*g*-PEtOx possessed the same PEtOx graft density while the adsorption of proteins decreased with the increase in the graft density of PEtOx when the chain length was fixed. The adsorption of proteins on PU-*g*-PEtOx was reduced by 97% compared with that on unmodified PU. The degradation of PU-*g*-PEtOx was monitored by a combination of ellipsometry and QCM-D because of the biodegradation of PCL segments. Furthermore, marine field tests were also performed during the rich fouling season and our results showed that PU-*g*-PEtOx exhibited much better anti-biofouling performance than unmodified PU.

Introduction

Nonspecific protein adsorption onto biomaterial surfaces has brought plenty of problems such as marine biofouling,[1] blood coagulation[2,3] and biological responses,[4,5] which lead to additional fuel cost and ship-renovation[6,7] as well as significant limitations of medical devices.[5] Protein-resistant coatings which are mainly based on the assumption that minimization of molecular adhesive forces between nonspecific proteins and coatings, such as biomimetic anti-fouling surfaces,[8–10] nanocomposites,[11] nanostructured surfaces,[12] hydrophilic surfaces,[13–20] zwitterionic polymers[21] and superhydrophic surfaces,[22] can be used to solve the protein adsorption problems.

Polyurethane (PU) is widely used in biofield research due to its good bio- and blood-compatibility[23,24] as well as easy modification.[25,26] PUs modified with different polymers especially hydrophilic polymers were widely investigated for protein resistance. For example, Zheng *et al.*[13] synthesized a series of L-tyrosine-derived polyurethanes with different molecular weights of poly(ethylene glycol) (PEG), and the PU films with PEG weight percentage higher than ~57% showed good low-fouling activity. Brash *et al.*[27,28] employed surface-initiated atom transfer radical graft polymerization (s-ATRgP) of poly[oligo(ethylene glycol) methacrylate] [poly(OEGMA)] to prepare protein-resistant polyurethane and found that the adsorbed amounts of fibrinogen and lysozyme decreased with increasing poly(OEGMA) chain length. They[29] further used the same method to obtain protein-resistant polyurethane with branched brushes by sequential grafting of poly(2-hydroxyethyl methacrylate) and poly(OEGMA) and got similar results. Francolini *et al.*[30] synthesized heparin-mimetic segmented polyurethanes, which can be used in the field of blood-contacting medical devices. Brady and Aronson[31] prepared fluorinated polyurethane films to control the nontoxic fouling ability. Four fluorinated elastomers were tested for fouling resistance during a full fouling season. Among them, PUs modified with hydrophilic polyethylene glycol (PEG) or oligo (ethylene glycol) (OEG) are effective to reduce protein adsorption,[13,27–29,32–34] presumably because the tightly bound water layer around the PEG chains can act as a "barrier" which can prevent the close approach of protein molecules according to "water barrier" hypothesis[35,36] or the compression of flexible PEG chains generates a repulsive interaction with an approaching protein according to "steric repulsion" hypothesis.[36,37]

Though PEG is one of the best candidates in biomaterials due to its biocompatibility, non-immunogenic and non-cytotoxic properties, it has been reported that PEG-containing coatings may lose their functions in complex biological fluids or in salt

[a]*Hefei National Laboratory for Physical Sciences at the Microscale, Department of Chemical Physics, University of Science and Technology of China, Hefei, Anhui 230026, China. E-mail: xdye@ustc.edu.cn*

[b]*Faculty of Materials Science and Engineering, South China University of Technology, Guangzhou 510640, China*

† Electronic supplementary information (ESI) available. See DOI: 10.1039/c6ra13663j

water and can undergo oxidative degradation leading to chain scission in the presence of oxygen and transition metal ions which exist in most biochemically relevant solutions.[38] These limitations push researchers to focus their researches on finding other bio-inert polymers which are usually hydrophilic and highly hydrated to replace PEG.[14,39,40] Once grafted onto a solid surface, they can prevent protein adsorption due to the mechanism mentioned above. Recently, poly(2-oxazoline)s have been introduced into the biofield[14–20,39,41–44] as a potential candidate since Déjardin *et al.*[45] first reported that poly(2-methyl-2-oxazoline)-*block*-poly(ethylene oxide)-*block*-poly(2-methyl-2-oxazoline) (PMeOx-*b*-PEO-*b*-PMeOx) triblock copolymer on silica particles can suppress platelet adhesion and fibrinogen adsorption. Pidhatika *et al.*[46] studied poly(L-lysine)-*graft*-poly(2-methyl-2-oxazoline) (PLL-*g*-PMeOx) copolymers adsorbed on Nb_2O_5 surface with different grafting densities, and the protein-resistant property of PMeOx brush was confirmed after exposure to human serum. Yan *et al.*[47] immobilized PEtOx with various molecular weights on silicon wafers and gold slides to form protein-resistant surfaces *via* photocoupling chemistry. Besides the excellent protein-resistant property, some groups have also compared poly(2-oxazoline)s with PEG in many aspects and confirm that poly(2-oxazoline)s show more advantages than PEG.[39,48–51] For example, Pidhatika *et al.*[51] investigated the stability of films with a dense brush layer of PEG or poly(2-methyl-2-oxazoline) (PMeOx), and they found that copolymer films grafted with PMeOx were significantly more stable than copolymer films grafted with PEG because PMeOx still retain its great protein-resistant property upon exposure to physiological conditions. Konradi *et al.*[39] reviewed a detailed comparison of PMeOx and PEG and concluded that PMeOx coatings showed higher stability than PEG in oxidative environment although both of them were equally excellent as anti-fouling surfaces.

Up to now, only few PUs modified with poly(2-oxazoline)s have been synthesized. For example, Shimano *et al.*[52] and Ronda *et al.*[53] mainly focused on the mechanical and thermal properties of poly-2-oxazoline-derived PUs; Kaku *et al.*[54] employed polyether urethane films coated with block copolymers of fluorinated oxazoline and 2-methyl-2-oxazoline to reduce the adsorption of fibrinogen and blood cells; Park *et al.*[55] employed PU films modified with hyperbranched PEtOx to enhance blood compatibility. However, most of these work focused on mechanical and thermal properties of poly(2-oxazoline)s as well as their biocompatibilities, less attention was paid to the non-specific protein resistance to different proteins. Furthermore, polymer architectures play an important role on their properties and polymer brushes[56] with side-chain structures are widely explored as anti-fouling surfaces because their better surface coverage through increased polymer density enhances protein resistance. But few of previous work explored brush-like PU with poly(2-oxazoline)s as side chains for protein resistance. Based on the superior characteristic of brush architecture, we designed degradable brush-like PUs for protein resistance. In detail, we chose biodegradable PCL as backbone and hydrophilic PEtOx as side chains due to its excellent properties as mentioned above to obtain renewable protein resistant coatings. A series of brush-like PU-*g*-PEtOx were synthesized and characterized by proton nuclear magnetic resonance (^{1}H NMR), Fourier transform infrared spectroscopy (FTIR) spectroscopy and gel permeation chromatography (GPC). The properties of the films such as the thickness, wettability and swelling behaviour were also studied. Furthermore, their nonspecific resistance to three different proteins including bovine serum albumin (BSA), lysozyme and fibrinogen was investigated by QCM-D and some of them showed excellent resistance to these proteins. Degradation behaviour of one PU-*g*-PEtOx film was also examined in the presence of lipase because of the degradation of PCL. The marine field tests were further performed and the results showed that PU modified with PEtOx exhibited better anti-biofouling performance than unmodified PU.

Experimental

Materials

Methyl tosylate (MeOTs, Alfa Aesar, 98%), 2-ethyl-2-oxazoline (EtOx, Alfa Aesar, 99%) were distilled over calcium hydride prior to use. Dihydroxyl functionalized polycaprolactone (HO-PCL-OH, Yichang Yongnuo Pharmaceutical Co., Ltd, 99%) and 1,4-butanediol (BDO, Alfa Aesar, 99%) was dried at 80 °C under vacuum for more than 2 h prior to use. Acetonitrile (ACN, Sinopharm, 99%) and triethylamine (NEt_3, Sinopharm, 99%) were refluxed over *p*-toluenesulfonyl chloride and then distilled over calcium hydride prior to use. Tetrahydrofuran (THF, Sinopharm, 99%) was dried with sodium and distilled prior to use. 4,4′-Methylenebis(phenyl isocyanate) (MDI, Alfa Aesar, 98%) and di-*n*-butyltin dilaurate (DBT, Alfa Aesar, 95%), fibrinogen [fraction I from human plasma, M_w = 340 kDa, isoelectric point (pI) = 5.5, Merck Chemicals], lysozyme *via* chicken eggwhite (Bio Basic Inc., >20 000 U mg^{-1}, M_w = 14.7 kg mol^{-1}, pI = 11.1), bovine serum albumin (BSA, Hualvyuan Biotechnology company, 98%, M_w = 68 kg mol^{-1}, pI = 4.8), 2,2-bis(hydroxymethyl)propionic acid (Sigma Aldrich, 98%), Amano Lipase PS (Sigma Aldrich, ≥30 000 U g^{-1}) were used as received. Physiological phosphate buffered saline with an ionic strength of 0.14 M at pH 7.4 was prepared by dissolving Na_2HPO_4 (Sinopharm, 99%) and KH_2PO_4 (Sinopharm, 99%) in Milli-Q water (Millipore, resistivity = 18.2 MΩ cm, 25 °C).

End-capping of living poly(2-ethyl-2-oxazoline) with 2,2-bis(hydroxymethyl)propionic acid

Dihydroxyl functionalized poly(2-ethyl-2-oxazoline) [PEtOx(OH)$_2$] was synthesized by cationic ring-opening polymerization and terminated with 2,2-bis(hydroxymethyl)propionic acid according to the references,[57,58] as shown in Scheme 1. In a typical experiment, EtOx (20.06 g, 202 mmol), MeOTs (1.88 g, 10 mmol), ACN (40 mL) were added to a 100 mL three-neck bottle. The solution was degassed by bubbling with argon for 30 min at room temperature to remove any trace of oxygen. Then the three-neck bottle was transferred to an oil bath at 80 °C and stirred for 24 h under argon atmosphere. 1 mL of reaction solution was taken out, precipitated into cold diethyl ether for twice and taken for ^{1}H-NMR after drying under vacuum at 45 °C for 24 h. Then 2,2-bis(hydroxymethyl)propionic acid (2.03 g, 15 mmol) and NEt_3

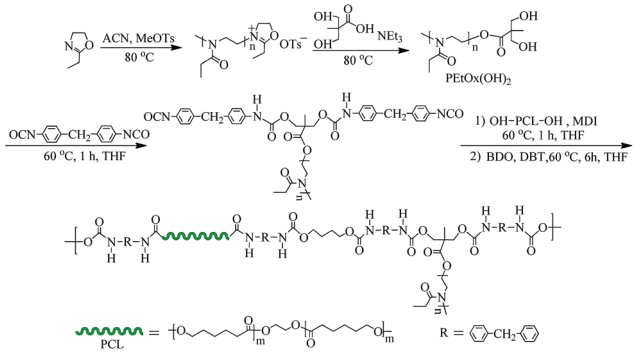

Scheme 1 Schematic of synthesis of polyurethane-*graft*-poly(2-ethyl-2-oxazoline) (PU-*g*-PEtOx) with HO-PCL-OH and PEtOx(OH)$_2$.

(2.02 g, 20 mmol) were subsequently added to the reaction mixture. After 15 h, the reaction was stopped and the solvent was removed by rotary evaporator. The product was redissolved in chloroform, washed with saturated aqueous sodium hydrogen carbonate and saturated brine. The organic phase was dried with sodium sulfate for more than 4 h, and then the filtrate was concentrated by rotary evaporator and precipitated into cold diethyl ether. The final product [PEtOx(OH)$_2$] (20 g, 93%) was white solid after drying under vacuum at 45 °C for 24 h. Thus, PEtOx(OH)$_2$ with different number-average molar masses (M_n) 0.98×10^3 g mol^{-1}, 2.02×10^3 g mol^{-1} and 3.18×10^3 g mol^{-1} were obtained and named as PEtOx(OH)$_2$-1K, PEtOx(OH)$_2$-2K and PEtOx(OH)$_2$-3K, respectively.

Synthesis of PU-*g*-PEtOx

PU-*g*-PEtOx was synthesized *via* a two-step process under argon atmosphere.[59] In a typical reaction for the synthesis of PU-*g*-PEtOx2K-0.5 (listed in Table 1), HO-PCL-OH (1.60 g, 0.8 mmol, $M_n = 2 \times 10^3$ g mol^{-1}) reacted with MDI (0.40 g, 1.6 mmol) in 5 mL THF and PEtOx(OH)$_2$ (0.92 g, 0.4 mmol) reacted with MDI (0.20 g, 0.8 mmol) in 5 mL THF separately at 60 °C for 1 h to yield two kinds of low-molecular-weight prepolymers, then these two prepolymers were mixed together. After 1 h, BDO (0.11 g, 1.2 mmol) and DBT (32 mg, 0.3 wt% based on the weight of the entire solution) were added as the chain extender and catalyst, respectively. Then the reaction continued at 60 °C for another 6 h. The mixture was precipitated into cold diethyl ether, rinsed with water and dried under vacuum at 45 °C for 24 h. PU-*g*-PEtOx with the same PCL length but different PEtOx chain lengths as well as various graft densities of PEtOx were synthesized according to the similar process. The feeding ratios of all the materials are listed in Table 1, where "2K" in PEtOx(OH)$_2$-2K means the value of M_n (about 2.0×10^3 g mol^{-1}) of PEtOx(OH)$_2$. For PU-*g*-PEtOx2K-0.5, "0.5" means the feeding ratio of PEtOx(OH)$_2$ to MDI when the feeding equivalent of MDI was fixed as 3.0. Other modified PUs with different M_n of PEtOx(OH)$_2$ and different feeding ratios are named with the same rule.

Characterization

Proton nuclear magnetic resonance spectroscopy (^{1}H NMR). ^{1}H NMR measurements were performed on a Bruker AV400 NMR spectrometer using deuterated chloroform $CDCl_3$ as solvent and tetramethylsilane (TMS) as internal standard. The polymer solutions had a concentration of ~20 g L^{-1}.

Table 1 Recipes for the synthesis of PU-*g*-PEtOx2K

	Molar ratios			
Different PUs	MDI	PEtOx(OH)$_2$-2K	HO-PCL-OH	BDO
PU	3.0	0	1.5	1.5
PU-*g*-PEtOx2K-0.5	3.0	0.5	1.0	1.5
PU-*g*-PEtOx2K-0.7	3.0	0.7	0.8	1.5
PU-*g*-PEtOx2K-0.9	3.0	0.9	0.6	1.5
PU-*g*-PEtOx2K-1.0	3.0	1.0	0.5	1.5

Fourier transform infrared spectroscopy (FTIR). FTIR spectra were performed on a Bruker VECTOR-22 IR spectrometer. The spectra of all samples were collected at 64 scans with a spectral resolution of 4 cm^{-1} by the KBr disk method.

Gel permeation chromatography (GPC). The molar mass and polydispersity index (PDI = M_w/M_n) were determined by Gel Permeation Chromatography (GPC, Waters 1515) equipped with three Waters Styragel columns (HR2, HR4, HR6) and a refractive index detector (RI, Wyatt WREX-02). THF was used as eluent at a flow rate of 1.0 mL min^{-1} and the column oven temperature was kept at 35 °C. Molar masses were calculated against a conventional universal calibration with linear polystyrene as standard.

Contact angle measurements. Contact angle measurements were performed employing a KSV (Helsinki, Finland) CAM 200 contact angle goniometer at 20 °C. The contact angle values were obtained by measuring different positions on each sample. Each measurement was taken at 2 seconds after the droplet contacted with the film. The measurement of each sample was repeated for six times.

Protein adsorption measurements by quartz crystal microbalance with dissipation (QCM-D). QCM-D and the AT-cut quartz crystals were from Q-sense AB. The films were spin-coated on Au wafer from THF solvent at a rotating speed of 2500 rpm for 20 seconds. The polymer concentration for all spin coatings was 1.0 g L^{-1} and the protein concentration for adsorption measurement was 1.0 g L^{-1}. Baseline measurements were taken after 30 minutes of equilibration of each module at 25 °C in the desired solution at a flow rate of 0.15 mL min^{-1} using a peristaltic pump. The quartz crystal resonator with a fundamental resonant frequency of 5 MHz was mounted in a fluid cell with one side exposed to the solution. The resonator has a mass sensitivity constant (C) of 17.7 ng cm^{-2} Hz^{-1}. The resonant frequency (Δf) is proportional to the mass change (Δm) of the layer. In vacuum or air, if the added layer is rigid, Δf is related to Δm and the overtone number ($n = 1, 3, 5\ldots$) by the Sauerbrey equation,[60,61]

$$\Delta m = -\frac{\rho_q l_q}{f_0}\frac{\Delta f}{n} = -C\frac{\Delta f}{n} \quad (1)$$

where f_0, ρ_q and l_q are the fundamental frequency, the specific density and thickness of the quartz crystal, respectively.

Thickness measurements. The thickness of polymer films was measured by a spectroscopic ellipsometry (M-2000V, J. A. Woollam, USA) at room temperature. The ellipsometric data were acquired where the incident angle were 70° and 80° in air and fit using Cauchy layer model to get the thickness of each polymer film.

Degradation measurements. Film made of PU-*g*-PEtOx2K-1.0 was used to examine the degradation property. The film was spin-coated on Au wafer from PU-*g*-PEtOx2K-1.0 THF solution with a concentration of 3.0 g L^{-1} at a rotating speed of 2500 rpm for 20 seconds. Degradation measurement was carried out in the presence of lipase with a concentration of 2.0 g L^{-1}. The process can be described as follows: polymer film was rinsed with Milli-Q water and dried in oven at 60 °C over 6 h after the Au wafer coated with PU-*g*-PEtOx2K-1.0 was immersed in lipase solution for predetermined hours. Then the dried Au wafer coated with polymer film was put back into lipase solution after the measurements of the frequency shift (Δf) by QCM-D and the polymer thickness by ellipsometry.

Swelling measurements. The kinetics of the swelling behaviour of the polymers was determined by dipping the polymer films in Milli-Q water at room temperature for different time periods. The percentage of swelling is given as the following equation:[30]

$$\text{Swelling}(\%) = \frac{m - m_0}{m_0} \times 100 \quad (2)$$

where m_0 is the initial weight of the film and m is the weight of the swollen film (dried with filter paper and then blew with N_2).

Marine field tests. The marine field tests were performed from May to August, at the inner Xiamen bay (24°45′N, 118°07′E) in China, where the marine biofouling is heavy because of the rich fouling organisms. The glass fiber reinforced epoxy resin panels (300 × 250 × 3 mm^3) coated with or without samples were lowered into seawater at depths of 0.2–2.0 m. In detail, panels coated with PU and PU-*g*-PEtOx2K-1.0 were tested, while the uncoated glass fiber reinforced epoxy resin panels were tested as control. At predetermined time, the panels were taken out of the sea, carefully washed with seawater and photographed, and then they were immediately placed back into the seawater to continue the test.

Results and discussion

As illustrated in Scheme 1, the synthetic process can be divided into two parts: (1) in the first part, PEtOx was prepared by cationic ring-opening polymerization for 24 h, subsequently terminated with 2,2-bis(hydroxymethyl)propionic acid. The end-capping reaction last for 15 h to furnish $PEtOx(OH)_2$. The whole procedure was under argon atmosphere and strictly in the absence of water; (2) in the second part, PU-*g*-PEtOx was prepared by polycondensation. $PEtOx(OH)_2$ and HO-PCL-OH were dehydrated at 80 °C under vacuum for more than 2 h prior to use and then reacted with MDI for 1 h at 60 °C to form –NCO terminated PU prepolymers, respectively. After combining the two kinds of prepolymers, chain extender and catalyst were added into the mixture to continue the reaction. The obtained PU-*g*-PEtOx solution was precipitated into cold diethyl ether and dried under vacuum at 45 °C for 24 h. The crude product PU-*g*-PEtOx was rinsed with water to remove any residue of unreacted $PEtOx(OH)_2$. Each intermediate product was characterized and conformed by several techniques (^{1}H NMR, GPC, FTIR).

Fig. 1 shows ^{1}H NMR spectra of PEtOx-3K, $PEtOx(OH)_2$-3K and PU-*g*-PEtOx3K-0.5. From the spectrum of PEtOx-3K in Fig. 1(a), chemical signal located at 3.3–3.6 ppm (signed as "c") is attributed to the protons from main chain backbone, and the signals located at 1–1.3 ppm (signed as "a") and 2.2–2.5 ppm (signed as "b") should be attributed to the protons from the side chains, respectively.[57] The signals located at 7.1–7.2 ppm and 7.6–7.7 ppm are attributed to protons H(*f*) and H(*e*) from the benzene ring, respectively. Therefore, the degree of polymerization of PEtOx (DP_{PEtOx}) was calculated according to the area ratio (A) of the two peaks from Fig. 1(a) as follows:

$$DP_{PEtOx} = 2A_a/3A_e \quad (3)$$

The polydispersity index (PDI) of PEtOx with different chain lengths determined by GPC are listed in Table 2 [$PEtOx(OH)_2$-3K], Table S1 [$PEtOx(OH)_2$-1K] and Table S2 [$PEtOx(OH)_2$-2K].† After the end-capping reaction, signals of the protons H(*e*) and H(*f*)

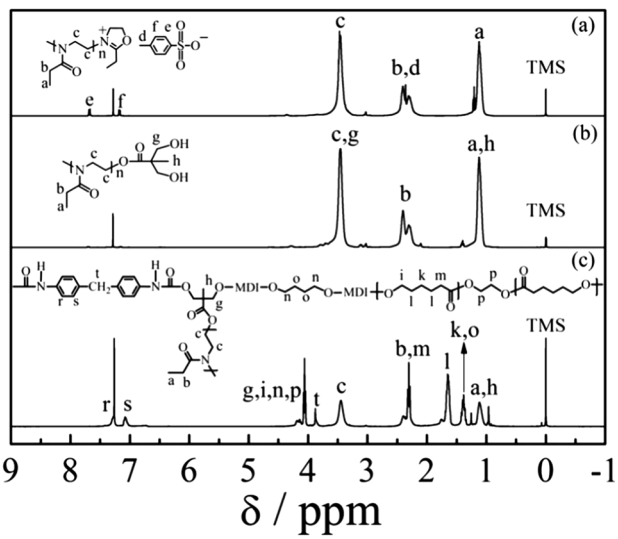

Fig. 1 ^{1}H NMR spectra of (a) PEtOx-3K, (b) $PEtOx(OH)_2$-3K and (c) PU-*g*-PEtOx3K-0.5.

Table 2 GPC results of $PEtOx(OH)_2$-3K and PU-*g*-PEtOx3K

Samples	M_n (g mol^{-1})	M_w (g mol^{-1})	PDI
$PEtOx(OH)_2$-3K	3.18×10^3	3.70×10^3	1.16
PU	5.59×10^4	1.15×10^5	2.06
PU-*g*-PEtOx3K-0.5	2.71×10^4	4.12×10^4	1.52
PU-*g*-PEtOx3K-0.7	2.01×10^4	3.93×10^4	1.96
PU-*g*-PEtOx3K-0.9	2.10×10^4	3.36×10^4	1.60
PU-*g*-PEtOx3K-1.0	1.65×10^4	2.43×10^4	1.47

from the end group almost disappear completely, as shown in Fig. 1(b). The substitution extent is evaluated to be over 95% according to the calculation from ^{1}H NMR. The characteristic signals belong to PCL and PEtOx are shown in Fig. 1(c) which demonstrate that the targeted polymer PU-*g*-PEtOx3K-0.5 was obtained.

GPC traces from RI detector of PEtOx(OH)$_2$ and PU-*g*-PEtOx with different chain lengths and various graft densities of PEtOx(OH)$_2$ are shown in Fig. 2, S1 and S2.† The PDI of all PEtOx(OH)$_2$ with different chain lengths are below 1.2, indicating living polymerization. After the co-polycondensation with HO-PCL-OH, the GPC peak shifts to lower retention time, as shown in Fig. 2, which indicates the successful synthesis of PU-*g*-PEtOx3K. Moreover, the molar mass of PU-*g*-PEtOx3K was smaller than PU without PEtOx(OH)$_2$, which may be attributed to the decreased activity because of the steric hindrance of PEtOx(OH)$_2$ chain.

Fig. 3 shows the FTIR spectra of PEtOx(OH)$_2$-3K, HO-PCL-OH and PU-*g*-PEtOx3K-0.5. Fig. 3(a) shows the detailed information of PEtOx(OH)$_2$-3K, the broad peak at 3500 cm^{-1} is ascribed to the stretching vibrations of terminal hydroxyls from PEtOx(OH)$_2$-3K, and the strong peak around 1640 cm^{-1} indicates the stretching vibrations of double bonds C=O from the PEtOx(OH)$_2$ backbone. The signals appearing at 1450 cm^{-1} and 2950 cm^{-1} are attributed to the bending vibrations and stretching vibrations of C–H.[62] The peak appearing at 1040 cm^{-1} is due to C–O stretching vibrations. Fig. 3(b) shows the detailed information of HO-PCL-OH, the strongest peak around 1750 cm^{-1} indicates the stretching vibrations of double bonds C=O from PCL main chain backbone. The peak at 1180 cm^{-1} is ascribed to C–O stretching vibrations. Fig. 3(c) shows the changes after the polycondensation. The intensity of the broad peak at 3500 cm^{-1} decreases, indicating the successful reaction of terminal hydroxyl groups from PEtOx(OH)$_2$ while another broad peak appearing around 3300 cm^{-1} can be attributed to the stretching vibrations of N–H from urethane amide bonds.[63] The appearance of peaks around 1640 cm^{-1} and 1750 cm^{-1} indicates stretching vibrations of double bonds C=O from the PEtOx(OH)$_2$ backbone and the double bonds from PCL backbone, respectively. Therefore, we confirm that we have successfully synthesized PU-*g*-PEtOx.

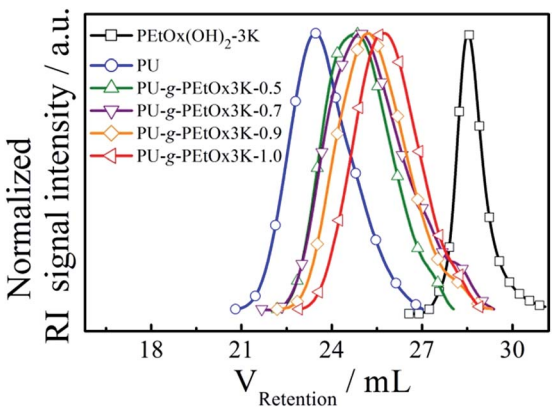

Fig. 2 GPC traces from RI detector of PEtOx(OH)$_2$-3K and PU-*g*-PEtOx3K with various graft densities of PEtOx(OH)$_2$-3K.

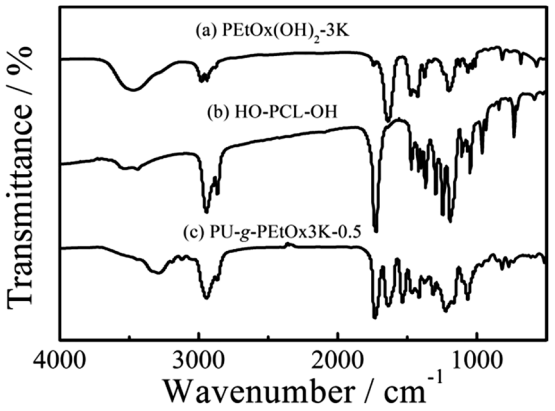

Fig. 3 FTIR spectra of (a) PEtOx(OH)$_2$-3K; (b) HO-PCL-OH; and (c) PU-*g*-PEtOx3K-0.5. The whole spectra are shown from 4000 to 500 cm^{-1}.

The protein resistance of PU and PU-*g*-PEtOx surfaces was further examined by QCM-D. Adsorption measurement of BSA was firstly studied because it is the most abundant protein in blood with a volume of 271 nm^3. As from Sauerbrey equation,[60] the increase in mass (Δm) on the sensor surface leads to the decrease of the frequency (Δf). Fig. 4 shows the time dependence of frequency shift (Δf) and dissipation shift (ΔD) for the adsorption of BSA on PU and PU-*g*-PEtOx3K surfaces at 25 °C. We can see that Δf for unmodified PU sharply decreases and then gradually levels off after BSA is introduced. Upon rinsing with PBS, Δf exhibits a marked decrease in comparison with the baseline for PBS, which demonstrates considerable adsorption of BSA on the unmodified PU surface. However, the modified PU-*g*-PEtOx shows less adsorption. Data for PU-*g*-PEtOx with various grafting densities demonstrate a negative correlation between the amount of BSA adsorption and the PEtOx grafting density which is in accord with Halperin's theory about the protein adsorption on polymer brushes[64] as well as the protein-resistant results of Brash *et al.*[27–29] For PU-*g*-PEtOx3K-0.9 and PU-*g*-PEtOx3K-1.0, the amount of adsorbed BSA was as low as 4 ng cm^{-2}.[27] Moreover, ΔD reflects the structure changes of polymer brushes,[61] and here the increase in ΔD relative to the baseline indicates that adsorbed BSA molecules form a viscoelastic layer. Fig. 4 clearly shows that ΔD is about 1.2×10^{-6} for unmodified PU and sharply decreases to 0.07×10^{-6} for PU-*g*-PEtOx3K-0.9, further indicating less adsorption of BSA on PU-*g*-PEtOx3K. Thus we can conclude that the BSA adsorption on PU-*g*-PEtOx3K is greatly reduced after PU was modified with PEtOx.

In order to investigate the resistance to other proteins, lysozyme and fibrinogen with different sizes and isoelectric points (PIs) are also used for adsorption measurements. Lysozyme is the smallest one among the three proteins with a volume of 27.6 nm^3, while fibrinogen is the largest one with a volume of 3645 nm^3.[32] The adsorption results of lysozyme and fibrinogen on PU-*g*-PEtOx3K studied by QCM-D are shown in Fig. S3 and S4.† Both of them have the same tendency with BSA adsorption.

PU-*g*-PEtOx with different PEtOx chain lengths and various PEtOx graft densities were used to study the effect of chain length on the protein resistance. The adsorption data of BSA, lysozyme and fibrinogen on PU-*g*-PEtOx1K and PU-*g*-PEtOx2K

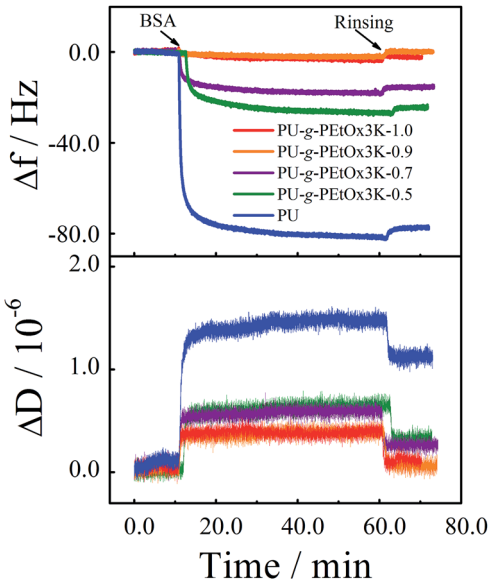

Fig. 4 Time dependence of frequency shift (Δ*f*) and dissipation shift (Δ*D*) for the adsorption of BSA on PU-*g*-PEtOx3K surfaces with various graft densities of $PEtOx(OH)_2$-3K at 25 °C.

studied by QCM-D are shown in Fig. S5–S10.† The final frequency shift (Δ*f*) for all measurements are summarized in Fig. 5. It can be seen that for most samples the adsorption of protein decreases with the increase in the PEtOx chain length when PU-*g*-PEtOx have the same graft density of PEtOx. When PU-*g*-PEtOx have the same PEtOx chain length but different graft densities of PEtOx, the adsorption of proteins decreases with the increase in PEtOx content. The adsorption of proteins on PU-*g*-PEtOx can be reduced by 97% compared with unmodified PU. Furthermore, the inhibition of adsorption on these surfaces is dependent on protein sizes to some extent, that is, the smallest lysozyme has the least adsorption, and the largest fibrinogen has the most adsorption. This may be presumably due to the different intermolecular interactions between these proteins and surfaces.

Wettabilities of PU and PU-*g*-PEtOx surfaces are investigated *via* contact angle measurements. Data of stationary water contact angle are illustrated in Fig. 6 for PU and PU-*g*-PEtOx2K with various graft densities where $PEtOx(OH)_2$-2K was employed. The contact angle for unmodified PU is about 80° which is in agreement with the literature.[52] The contact angles of all PU-*g*-PEtOx modified with PEtOx are smaller than that of unmodified PU, and decrease with the increase in PEtOx content which indicates enhanced hydrophilic property. The strong hydrophilic property of the polymer can improve the capacity for the inhibition of adsorption because the hydrophilic surface can form a stable hydration layer to inhibit the adsorption of hydration protein as hydration theory described.[65] Data for PU-*g*-PEtOx1K and PU-*g*-PEtOx3K are illustrated in Fig. S11 and S12.† Both of them show a similar tendency.

Swelling behaviour of polymer films is an important parameter to affect their anti-fouling properties. The approach of protein towards hydrated PEG chains will lead to repulsive

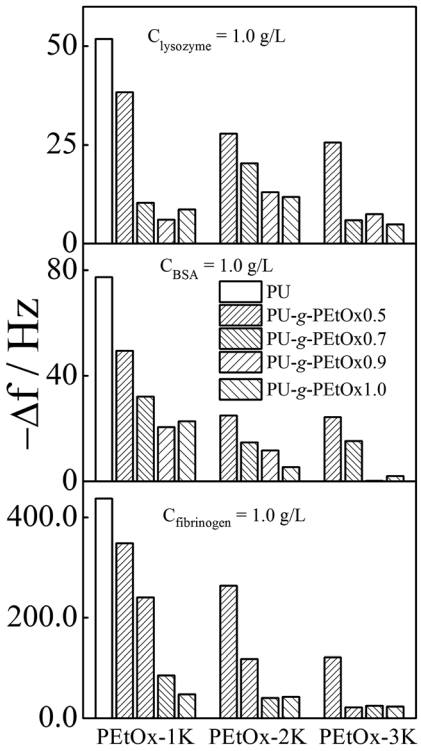

Fig. 5 The final frequency shift (Δ*f*) for the adsorption of three different proteins on polymeric surfaces at 25 °C. The concentration of all proteins used in the adsorption measurements was 1.0 g L^{-1}.

elastic forces and the removal of water molecules from the hydrated polymer is a thermodynamically unfavourable state.[44,66] Therefore, the swelling behaviour of PU-*g*-PEtOx2K was also examined due to the hydrophilic property of PEtOx. It's well known that swelling ratio is associated with backbone structure and their functional groups. It has been reported[30] that there are two kinds of adsorbed water: one entrapped in the accessible interspaces between the polymers, which causes polymer swelling, while the other interacts with the polymer

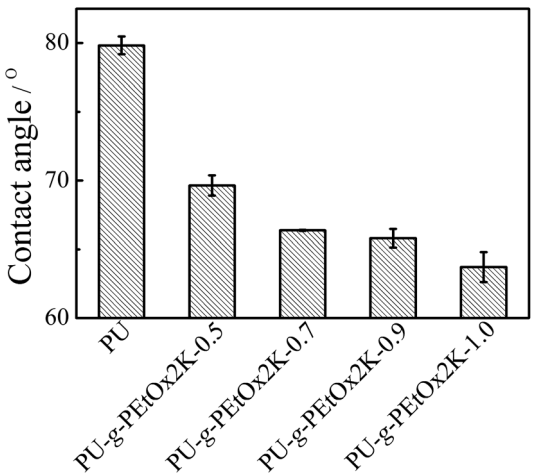

Fig. 6 Stationary water contact angle of PU and PU-*g*-PEtOx2K with various graft densities where the $PEtOx(OH)_2$-2K was employed.

chains through hydrogen bond interactions. The introduction of the hydrophilic segment PEtOx significantly influenced the swelling ability of PU-*g*-PEtOx because PEtOx chain can strongly interact with water through hydrogen bond interactions.[39] The swelling kinetics of PU and PU-*g*-PEtOx2K with various graft densities where PEtOx(OH)$_2$-2K was used was studied and data are shown in Fig. 7. In particular, the swelling ratio of PU-*g*-PEtOx possesses a positive correlation with the amount of PEtOx. PU's swelling ratio is about only 30%, while the PU-*g*-PEtOx2K-1.0 has the biggest swelling ratio around 150%, indicating the hydrophilic property of PU-*g*-PEtOx.

It is well known that aliphatic polyester PCL is biodegradable.[67,68] Degradation process of PU-*g*-PEtOx2K-1.0 coated on Au wafer was examined in the presence of lipase. Fig. 8 shows the degradation kinetic curve of PU-*g*-PEtOx2K-1.0. The degradation process was detected with QCM-D and ellipsometer respectively. To accelerate the degradation velocity in laboratory condition, the degradation temperature was set at 50 °C which is the optimal temperature for lipase. The data were obtained at 0 h, 1 h, 2 h, 4 h, 8 h, 12 h, 17 h and 22 h. At the beginning, the thickness was 22.5 nm measured by ellipsometer and the frequency shift (Δf) was set as 0 Hz. As shown in Fig. 8, Δf increases with time after PU-*g*-PEtOx2K-1.0 film is immersed in lipase solution, indicating the mass loss of the film. On the other hand, the thickness of the polymer turns to be thinner with time as evident from the data of ellipsometer in Fig. 8. The degradation process is almost finished after 8 h. The frequency and polymer thickness gradually levels off after 12 h. According to Rutkowska *et al.*,[69] the PU–PCL (38% hard segment) has a moderate degradation velocity (4.2% mass loss after 12 months), and Kim *et al.*[70] found that PU–PCL with less hard segment content is more biodegradable. In our experiment, PU-*g*-PEtOx2K-1.0 with less hard segment content (22.8%) is supposed to degrade faster than Rutkowska's sample and the high degradation temperature also contributes to the faster degradation. Furthermore, the final thickness is around 4 nm, presumably due to the lipase film adsorbed on the Au wafer after the PCL segments in PU-*g*-PEtOx were completely degraded.

We also explored the anti-biofouling of the modified PU by marine field tests. The results were displayed in Fig. 9. After 30 days, both of bare epoxy resin panel and PU coated panel have some juvenile barnacles grown on their surfaces. There is no visible difference between them. However, there is scarcely any barnacle located on the panel coated with PU-*g*-PEtOx2K-1.0. After 90 days of exposure in marine environment, the bare epoxy resin panel and PU coated panel are extremely fouled. The panel coated with PU-*g*-PEtOx2K-1.0 is also slightly fouled. The numbers of marine organism grown on the panels are listed in Fig. 9(b). However, the PU-*g*-PEtOx2K-1.0 surface remains clean for 30 days and it is reasonable anti-biofouling for 60 days. Two factors may be account for the anti-fouling properties of PU-*g*-PEtOx2K-1.0. One is the protein resistance of PEtOx chain because the attachment of some marine organisms *via* byssal threads and adhesive plaques formed from a composite of several proteins,[1] the other is the degradation of PU-*g*-PEtOx2K-1.0 making the film renewable.[63] As we know, the marine environment is an extremely complicated system, and there is no uniform adsorption mechanism for all marine creatures.

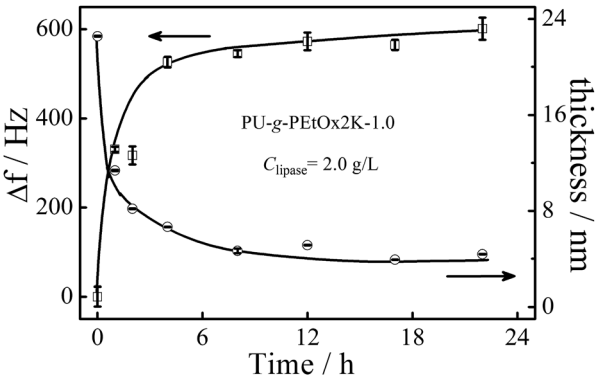

Fig. 8 Time dependence of the frequency shift (Δf) and the polymer thickness on Au wafer when PU-*g*-PEtOx2K-1.0 was immersed in lipase solution with a concentration 2.0 g L^{-1}.

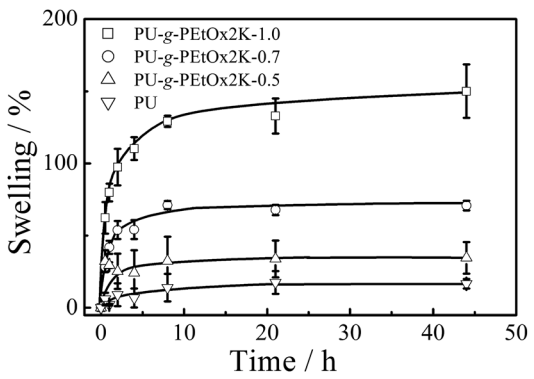

Fig. 7 Time dependence of swelling ratio of PU and PU-*g*-PEtOx2K with various graft densities where the PEtOx(OH)$_2$-2K was used.

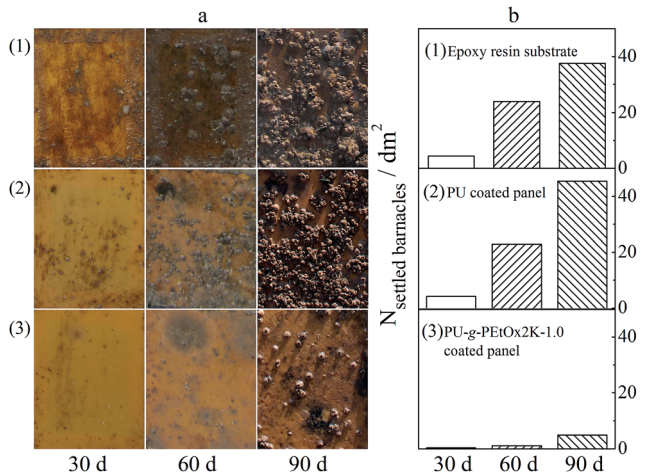

Fig. 9 The results of marine field tests: (a) images of (1) bare epoxy resin panels as control, (2) panels coated with PU and (3) panels coated with PU-*g*-PEtOx2K-1.0; (b) the numbers of marine organism grown on the panels after immersion in seawater for predetermined time (May–August, Xiamen, China).

Thus much effort is still needed to modify the properties of the film and to improve the bio-antifouling or biocides might be added in the PU films to increase the anti-fouling properties.

Conclusions

A series of PU-*g*-PEtOx with various PEtOx graft densities as well as different PEtOx chain lengths were prepared through polycondensation. Several measurements (^{1}H NMR, GPC, FTIR) were employed to confirm the structures of the obtained PU-*g*-PEtOx. Nonspecific protein resistance properties were studied by QCM-D and three proteins (BSA, lysozyme and fibrinogen) with different sizes were used. From QCM-D results, we confirm that higher PEtOx graft density and relatively longer PEtOx chain length lead to less protein adsorption. The adsorption of proteins on PU-*g*-PEtOx was reduced by 97% compared with unmodified PU. We also confirm that the inhibition of adsorption on these surfaces is dependent on protein size to some extent. The adsorption possessed a positive correlation with the protein size, and all surfaces showed the most adsorption for fibrinogen when compared with two other proteins. It's worth noting that PCL was used to make PU degradable in our study because the renewable coating can maintain its anti-fouling property for a long period of time. Furthermore, the marine field tests were performed during the rich fouling season from May to August. PU-*g*-PEtOx2K-1.0 exhibited much better anti-biofouling performance than unmodified PU.

Acknowledgements

We thank Prof. Guangzhao Zhang for his kind assistance during the experiments. The financial support of the National Program on Key Basic Research Project (2012CB933800), the National Natural Scientific Foundation of China (NNSFC) Projects (21274140) and the Fundamental Research Funds for the Central Universities (WK2340000066) is gratefully acknowledged.

References

1 J. A. Callow and M. E. Callow, *Nat. Commun.*, 2011, **2**, 244.
2 J. L. Brash, *J. Biomater. Sci., Polym. Ed.*, 2000, **11**, 1135.
3 J. H. Lee, Y. M. Ju and D. M. Kim, *Biomaterials*, 2000, **21**, 683.
4 P. Thomsen and C. Gretzer, *Curr. Opin. Solid State Mater. Sci.*, 2001, **5**, 163.
5 J. M. Anderson, *Annu. Rev. Mater. Res.*, 2001, **31**, 81.
6 M. P. Schultz, *Biofouling*, 2007, **23**, 331.
7 M. P. Schultz, J. A. Bendick, E. R. Holm and W. M. Hertel, *Biofouling*, 2011, **27**, 87.
8 J. Zheng, W. Song, H. Huang and H. Chen, *Colloids Surf., B*, 2010, **77**, 234.
9 M. L. Carman, T. G. Estes, A. W. Feinberg, J. F. Schumacher, W. Wilkerson, L. H. Wilson, M. E. Callow, J. A. Callow and A. B. Brennan, *Biofouling*, 2006, **22**, 11.
10 S. Nir and M. Reches, *Curr. Opin. Biotechnol.*, 2016, **39**, 48.
11 A. Beigbeder, P. Degee, S. L. Conlan, R. J. Mutton, A. S. Clare, M. E. Pettitt, M. E. Callow, J. A. Callow and P. Dubois, *Biofouling*, 2008, **24**, 291.
12 E. Martinelli, S. Agostini, G. Galli, E. Chiellini, A. Glisenti, M. E. Pettitt, M. E. Callow, J. A. Callow, K. Graf and F. W. Bartels, *Langmuir*, 2008, **24**, 13138.
13 J. C. Yang, C. Zhao, I. F. Hsieh, S. Subramanian, L. Y. Liu, G. Cheng, L. Y. Li, S. Z. D. Cheng and J. Zheng, *Polym. Int.*, 2012, **61**, 616.
14 R. Konradi, B. Pidhatika, A. Mühlebach and M. Textor, *Langmuir*, 2008, **24**, 613.
15 B. Pidhatika, J. Möller, V. Vogel and R. Konradi, *Chimia*, 2008, **62**, 264.
16 R. Hoogenboom, *Angew. Chem., Int. Ed.*, 2009, **48**, 7978.
17 X. J. Zheng, C. Zhang, L. C. Bai, S. T. Liu, L. Tan and Y. M. Wang, *J. Mater. Chem. B*, 2015, **3**, 1921.
18 C. Zhang, S. T. Liu, L. Tan, H. K. Zhu and Y. M. Wang, *J. Mater. Chem. B*, 2015, **3**, 5615.
19 A. A. Cavallaro, M. N. Macgregor-Ramiasa and K. Vasilev, *ACS Appl. Mater. Interfaces*, 2016, **8**, 6354.
20 T. He, D. Jańczewski, S. Jana, A. Parthiban, S. F. Guo, X. Y. Zhu, S. S.-C. Lee, F. J. Parra-Velandia, S. L.-M. Teo and G. J. Vancso, *J. Polym. Sci., Part A: Polym. Chem.*, 2016, **54**, 275.
21 S. Y. Jiang and Z. Q. Cao, *Adv. Mater.*, 2010, **22**, 920.
22 J. Genzer and K. Efimenko, *Biofouling*, 2006, **22**, 339.
23 T. G. Grasel and S. L. Cooper, *Biomaterials*, 1986, **7**, 315.
24 R. J. Zdrahala and I. J. Zdrahala, *J. Biomater. Appl.*, 1999, **14**, 67.
25 L. Xue and H. P. Greisler, *J. Vasc. Surg.*, 2003, **37**, 472.
26 D. Fournier and F. Du Prez, *Macromolecules*, 2008, **41**, 4622.
27 Z. L. Jin, W. Feng, S. P. Zhu, H. Sheardown and J. L. Brash, *J. Biomed. Mater. Res., Part A*, 2009, **91**, 1189.
28 Z. L. Jin, W. Feng, K. Beisser, S. P. Zhu, H. Sheardown and J. L. Brash, *Colloids Surf., B*, 2009, **70**, 53.
29 Z. L. Jin, W. Feng, S. P. Zhu, H. Sheardown and J. L. Brash, *J. Biomed. Mater. Res., Part A*, 2010, **95**, 1223.
30 I. Francolini, F. Crisante, A. Martinelli, L. D'Ilario and A. Piozzi, *Acta Biomater.*, 2012, **8**, 549.
31 R. F. Brady and C. L. Aronson, *Biofouling*, 2003, **19**, 59.
32 J. G. Archambault and J. L. Brash, *Colloids Surf., B*, 2004, **33**, 111.
33 J. G. Archambault and J. L. Brash, *Colloids Surf., B*, 2004, **39**, 9.
34 J. Yang, J. Lv, M. Behl, A. Lendlein, D. Z. Yang, L. Zhang, C. C. Shi, J. T. Guo and Y. K. Feng, *Macromol. Biosci.*, 2013, **13**, 1681.
35 K. L. Prime and G. M. Whitesides, *Science*, 1991, **252**, 1164.
36 S. F. Chen, F. C. Yu, Q. M. Yu, Y. He and S. Y. Jiang, *Langmuir*, 2006, **22**, 8186.
37 S. I. Jeon, J. H. Lee, J. D. Andrade and P. G. De Gennes, *J. Colloid Interface Sci.*, 1991, **142**, 149.
38 Z. Zhang, J. A. Finlay, L. F. Wang, Y. Gao, J. A. Callow, M. E. Callow and S. Y. Jiang, *Langmuir*, 2009, **25**, 13516.
39 R. Konradi, C. Acikgoz and M. Textor, *Macromol. Rapid Commun.*, 2012, **33**, 1663.
40 E. W. Merrill, *Ann. N. Y. Acad. Sci.*, 1987, **516**, 196.

41 H. Schlaad, C. Diehl, A. Gress, M. Meyer, A. L. Demirel, Y. Nur and A. Bertin, *Macromol. Rapid Commun.*, 2010, **31**, 511.
42 R. Luxenhofer, Y. C. Han, A. Schulz, J. Tong, Z. J. He, A. V. Kabanov and R. Jordan, *Macromol. Rapid Commun.*, 2012, **33**, 1613.
43 N. Zhang, T. Pompe, I. Amin, R. Luxenhofer, C. Werner and R. Jordan, *Macromol. Biosci.*, 2012, **12**, 926.
44 L. Tauhardt, K. Kempe, M. Gottschaldt and U. S. Schubert, *Chem. Soc. Rev.*, 2013, **42**, 7998.
45 C. Maechling-Strasser, P. Déjardin, J. C. Galin, A. Schmitt, V. Housse-Ferrari, B. Sébille, J. N. Mulvihill and J. P. Cazenave, *J. Biomed. Mater. Res.*, 1989, **23**, 1395.
46 B. Pidhatika, Y. Chen, G. Coullerez, S. Al-Bataineh and M. Textor, *Anal. Bioanal. Chem.*, 2014, **406**, 1509.
47 H. Wang, L. L. Li, Q. Tong and M. D. Yan, *ACS Appl. Mater. Interfaces*, 2011, **3**, 3463.
48 A. Mero, G. Pasut, L. D. Via, M. W. M. Fijten, U. S. Schubert, R. Hoogenboom and F. M. Veronese, *J. Controlled Release*, 2008, **125**, 87.
49 O. Sedlacek, B. D. Monnery, S. K. Filippov, R. Hoogenboom and M. Hruby, *Macromol. Rapid Commun.*, 2012, **33**, 1648.
50 C. Weber, R. Hoogenboom and U. S. Schubert, *Prog. Polym. Sci.*, 2012, **37**, 686.
51 B. Pidhatika, M. Rodenstein, Y. Chen, E. Rakhmatullina, A. Mühlebach, C. Acikgöz, M. Textor and R. Konradi, *Biointerphases*, 2012, **7**, 1.
52 Y. Shimano, K. Sato, M. Yoshida and S. Narumi, *Polym. J.*, 1999, **31**, 687.
53 E. Del Rio, G. Lligadas, J. C. Ronda, M. Galià and V. Cádiz, *J. Polym. Sci., Part A: Polym. Chem.*, 2011, **49**, 3069.
54 M. Kaku, L. C. Grimminger, D. Y. Sogah and S. L. Haynie, *J. Polym. Sci., Part A: Polym. Chem.*, 1994, **32**, 2187.
55 Y. S. Park, Y. S. Kang and D. J. Chung, *e-Polym.*, 2002, **2**, 211.
56 G. Gunkel, M. Weinhart, T. Becherer, R. Haag and W. T. S. Huck, *Biomacromolecules*, 2011, **12**, 4169.
57 C. Weber, C. R. Becer, A. Baumgaertel, R. Hoogenboom and U. S. Schubert, *Des. Monomers Polym.*, 2009, **12**, 149.
58 C. Weber, C. R. Becer, W. Guenther, R. Hoogenboom and U. S. Schubert, *Macromolecules*, 2010, **43**, 160.
59 C. F. Ma, H. Zhou, B. Wu and G. Z. Zhang, *ACS Appl. Mater. Interfaces*, 2011, **3**, 455.
60 G. Sauerbrey, *Z. Phys.*, 1959, **155**, 206.
61 T. Wang, X. W. Wang, Y. C. Long, G. M. Liu and G. Z. Zhang, *Langmuir*, 2013, **29**, 6588.
62 K. M. Zia, M. Barikani, M. Zuber, I. A. Bhatti and M. A. Sheikh, *Carbohydr. Polym.*, 2008, **74**, 149.
63 C. F. Ma, L. G. Xu, W. T. Xu and G. Z. Zhang, *J. Mater. Chem. B*, 2013, **1**, 3099.
64 A. Halperin, *Langmuir*, 1999, **15**, 2525.
65 S. Krishnan, C. J. Weinman and C. K. Ober, *J. Mater. Chem.*, 2008, **18**, 3405.
66 I. Banerjee, R. C. Pangule and R. S. Kane, *Adv. Mater.*, 2011, **23**, 690.
67 C. G. Pitt, F. I. Chasalow, Y. M. Hibionada, D. M. Klimas and A. Schindler, *J. Appl. Polym. Sci.*, 1981, **26**, 3779.
68 G. G. Pitt, M. M. Gratzl, G. L. Kimmel, J. Surles and A. Schindler, *Biomaterials*, 1981, **2**, 215.
69 M. Rutkowska, K. Krasowska, A. Heimowska, I. Steinka and H. Janik, *Polym. Degrad. Stab.*, 2002, **76**, 233.
70 Y. D. Kim and S. C. Kim, *Polym. Degrad. Stab.*, 1998, **62**, 343.